INSTITUTE OF PHYSICS PUBLISHING SUPERCONDUCTOR SCIENCE AND TECHNOLOGY
Supercond. Sci. Technol. 14 (2001) 685–689 PII: S0953-2048(01)26375-1

Scanning potentiometry and magnetic imaging of current transport in high-temperature superconductor coated conductors

G K Perkins, Yu V Bugoslavsky and A D Caplin

Blackett Laboratory, Imperial College of Science Technology and Medicine, Prince Consort Road, London SW7 2BZ, UK

Received 4 June 2001
Published 16 August 2001
Online at stacks.iop.org/SUST/14/685

Abstract

Second generation $Y_1Ba_2Cu_3O_{7-\delta}$ (YBCO) coated conductors promise greater performance than first generation powder-in-tube technology. Along with the development of these materials, advances in characterization techniques have enabled detailed studies of current flow, grain boundaries and homogeneity. We have developed a scanning probe system which can be configured to map either the magnetic field or electric potential at the sample surface (with a local Hall sensor or voltage probe respectively). While the magnetic image can be used to determine the current flow pattern, the potential map allows direct measurement of the local dissipation within the samples.

1. Introduction

The complex microstructure of high-temperature superconductors (HTSs) has driven the development of local characterization techniques for the study of their electrodynamics. Techniques for imaging the magnetic field $\boldsymbol{B}$ at the sample surface have been widely used to extract information on the local current flow in the samples [1, 2]; but comparatively little has been done on to measure the local *electric* field $\boldsymbol{E}$, although in principle, when combined with $\boldsymbol{B}$, this allows direct study of the local dissipation. For inhomogeneous nonlinear media (such as HTSs) modelling this problem is non-trivial [3]. In this paper we discuss measurements of both the local fields $\boldsymbol{B}$ and $\boldsymbol{E}$ in HTS coated conductors using a scanning Hall sensor and scanning voltage probe, respectively.

2. Experiment

We present measurements of both magnetic and electric field profiles generated by a transport current passing through samples which have been patterned into a short bridge geometry using a diamond scribe (figure 1). Two samples have been studied, the first sample S (to denote 'superconducting') is a $Yba_2Cu_3O_{7-\delta}$ film of dimensions 3×8 mm^2 and thickness 300 nm, deposited on sapphire by thermal evaporation, with a 50 nm Au capping layer (which is important for the potentiometry measurements as it allows for good electrical contact with the Au plated tip). This sample has a critical current density J_c of 2 MA cm^{-2} at 77 K.

The second sample N (denoting 'normal') is a Cu film of dimensions 8×8 mm^2 and thickness 50 μm. Measurements on sample S are performed at 77 K while for N they are at room temperature.

2.1. Magnetic imaging

Magnetic images were obtained using a scanning Hall probe technique, implementing a 50 μm InSb Hall bar with a sensitivity of order 1 μT Hz$^{-1/2}$. Details the scanning technique are given elsewhere [4].

2.2. Scanning potentiometry

Mapping of the electric potential is achieved by replacing the Hall sensor with a point contact (a gold plated sphere of radius ~500 μm). The tip is then brought into light contact with the sample at each point in order to construct the electric image. After each contact, the tip is lifted a small distance (~50 μm) before being moved to the next position, thus minimizing surface damage due to friction.

0953-2048/01/090685+05$30.00

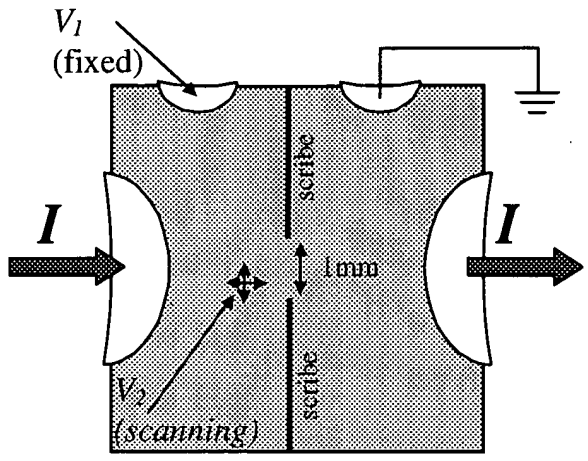

Figure 1. Both samples are patterned into a short bridge of width ~1 mm. A transport current is passed through the bridge while voltages at V_1 and V_2 can be measured. V_1 remains fixed and serves as a global $I-V$ measurement. V_2 is scanned in the plane to measure the local potential map.

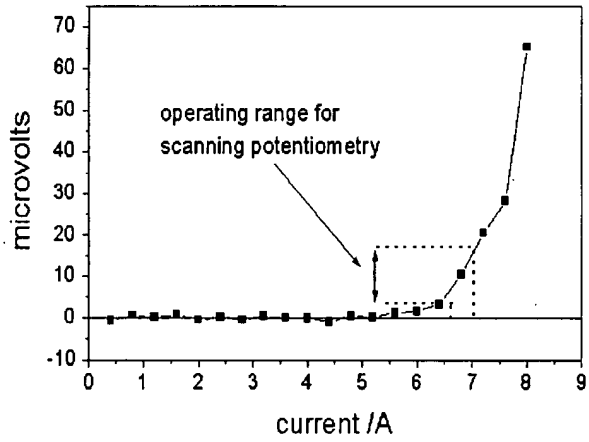

Figure 2. Global $I-V$ characteristic of sample S at 77 K, used to determine an appropriate transport current for the scanning potentiometry measurements. It can be seen that a 6.5 A dc current with an additional 0.5 A square-wave ripple will switch the voltage between 0 μV and 15 μV. The curve approximately obeys a power law with an exponent of 26–30.

In order to avoid problems of thermal e.m.f.'s and drift during the measurements, the experiment was performed using a quasi ac current, whereby a small square-wave ripple current (0.5 A, 20 Hz) is added to the dc current. Because of the highly nonlinear nature of the current–voltage ($I-V$) characteristics, the relatively small ac component of the current can be made to modulate effectively 100% of the voltage, so that the signal can be measured using ac detection techniques. To achieve this, the dc current level is chosen to be that at which a measurable voltage is first detected across the sample. In figure 2 it can be seen that for sample S this is 6.5 A, and that the additional 0.5 A ac component switches the voltage between 0 V and 15 μV. It should be stressed that at these relatively high electric field values (at least 15 μV cm^{-1}), the transients associated with flux redistribution [5] occur on a much shorter time scale than the period of the ac cycle (50 ms) so that the experiment can essentially be considered to be in the dc limit.

Figure 3. (a) Electric potential image for a transport current of 0.5 A ac, (some distance away from the bridge) for sample S at room temperature. The grey scale spans a 2 μV range. The black dots represent points where no contact could be made with the sample; this occurs less then 10% of the time. (b) Corresponding image after the sample was cooled to 77 K by immersion into liquid nitrogen. The grey scale spans a 2 μV range. The black dots again represent points where no contact could be made with the sample; this occurs more than 90% of the time. (c) Image taken directly after that in (b) but with a 9 V bias applied to the tip. This allows a good contact to be made more than 90% of the time. Here the grey scale spans a 100 nV range. Each image represents an area of 2 mm $\times$ 2 mm.

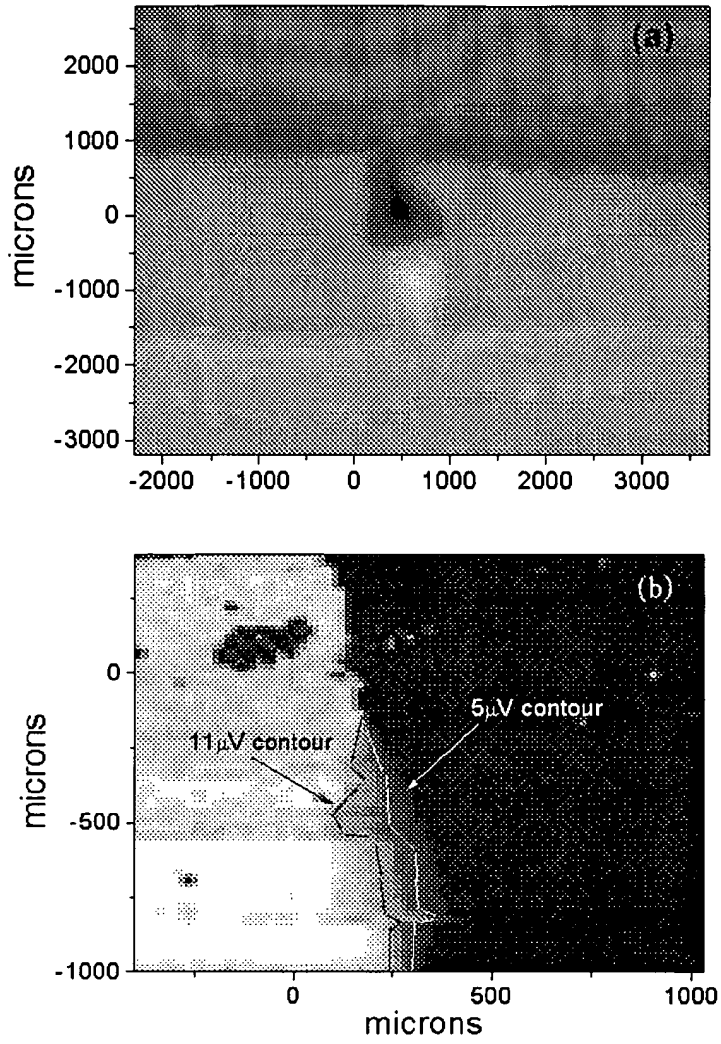

Figure 4. (a) Magnetic flux profile of sample S at 77 K generated by a transport current of 7 A (here the grey scale represents a magnetic field range of -6 mT $< B <$ 6 mT). The flux penetrates at the edges of the sample and along the sides of the bridge; the flux fronts meet at the centre of the bridge. (b) Electric potential image for a transport current of 7 A (6.5 A + 0.5 A square-wave ripple) in the vicinity of the bridge for sample S at 77 K (the grey scale represents an electric potential range of 0 μV $< V <$ 16 μV). Equipotentials represent lines of vortex flow, which are confined to a narrow plume connecting the bridge. Note that the origins of the x–y scales in the two images do not coincide.

We have used a contact force of ~100 mN throughout. This we find is small enough so that no measurable degradation of the global electrical characteristics was detected after a complete scan was performed. Nor was any visible surface damage apparent when viewed under an optical microscope at ×50 magnification. At room temperature the force was sufficient to a make good electrical contact with the sample most of the time, as can be seen from the potential map in figure 3(a), where more than 90% of the pixels in the image are good. However, figure 3(b) shows that after the sample was cooled to 77 K by immersion in liquid nitrogen, it became very difficult to make a contact and less than 10% of the pixels are good. We have not been able to establish the precise reason for this degredation in the sample surface, although it is most likely to be due to a layer of adsorbed water which is known to occur readily under most conditions.

We have found that a good way to alleviate the problem is to apply a bias voltage to the tip. A large impedance limits the current through the tip to ~1 μA, small enough so as not to damage the tip but sufficient to breakdown the surface layer and make an electrical contact. This is shown by the image figure 3(c), which was taken directly after that of figure 3(b) but with a 9 V bias on the tip. Here, a good contact is made most of the time, although there are visibly some bad areas of the sample where it was not possible to make a contact. Although the bias current will produce a varying offset voltage depending on the value of the contact resistance at each point in the image, this will not effect the measurement as only the ac component of the voltage is detected,

With this technique we achieve input noise levels of 6 nV $Hz^{-1/2}$ at zero current (equal to the input noise of our lock-in amplifier). However pixel-to-pixel fluctuations in the final image can be significantly greater than this and may be due to drift in the applied transport current.

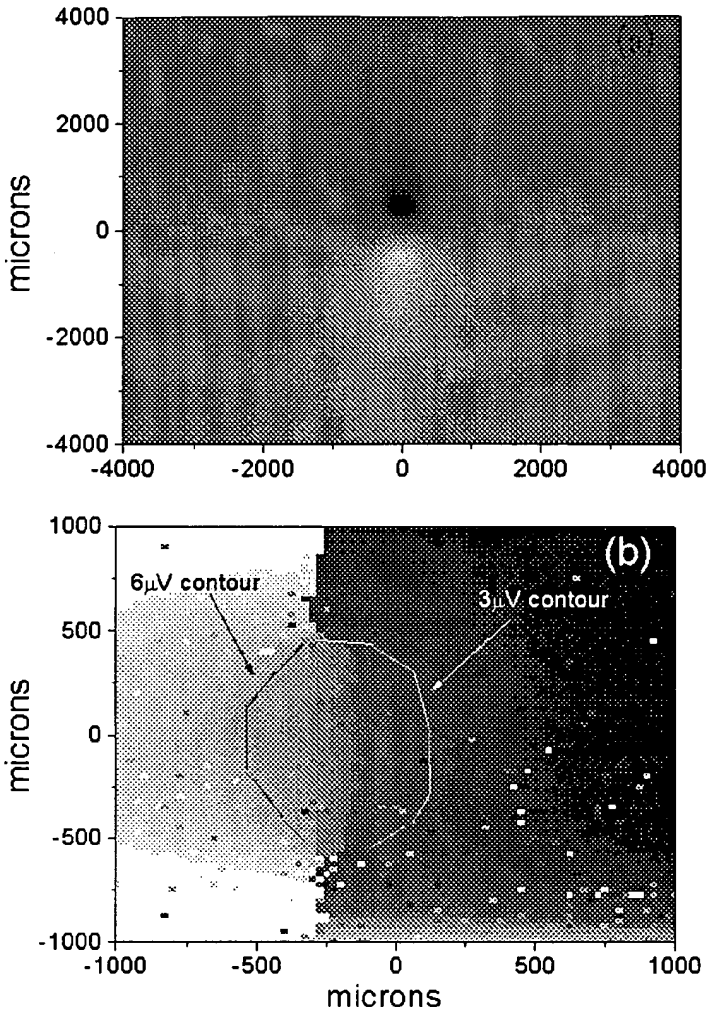

Figure 5. (a) Magnetic flux profile of sample N at 77 K generated by a transport current of 0.5 A (here the grey scale represents a magnetic field range of -0.8 mT $< B <$ 0.8 mT). Flux is concentrated around the area of the bridge. (b) Corresponding image of the electric potential for a 0.5 A square-wave transport current (no dc component) in the vicinity of the bridge (the grey scale represents an electric potential range of 0 μV $< V <$ 10 μV). The electric field channel displays no obvious eccentricity in contrast to the superconducting case. Note that the origins of the x–y scales in the two images do not coincide.

3. Results

Magnetic images were made for both samples over an area of 8×8 mm^2 with a resolution of order 50 μm, while in the case of the electric images the scanned area was 2×2 mm^2 with a resolution of 25 μm. The superconducting and ohmic cases are presented separately below.

3.1. Superconducting case

The measured magnetic field and electric potential maps for sample S at 77 K are shown in figures 4(a) and (b) respectively. In figure 4(a) the magnetic flux (arising from the applied transport current) is screened over most of the sample and only penetrates near to the edges; the flux fronts meet only in the centre of the bridge. Figure 4(b) shows that changes in electric potential (i.e. the electric field) are confined to a narrow 'plume', which connects the two ends of the bridge. Elementary electromagnetism requires that the equipotentials within this plume represent lines of vortex flow. Two such lines at 5 μV and 11 μV (spanning approximately one-third of the total voltage range) are indicated in the figure and approximately form an ellipse of eccentricity of five to ten.

3.2. Ohmic case

The magnetic image for the ohmic sample N is shown in figure 5(a). In contrast to the superconducting case the flux density is uniform except in the vicinity of the bridge. This reflects that there is no magnetic shielding for the ohmic case, and the current distributes itself more uniformly over the sample. However, it is necessarily concentrated at the narrow channel of the bridge in order to maintain current continuity.

The image of the electric potential, figure 5(b), shows a region of high electric field around the bridge, similar to the superconducting case, but no clear eccentricity is observed.

4. Discussion

The focus of this discussion is on the shape of the electric field region around the bridge and its relation the $I-V$ characteristic of the conducting medium. In a recent paper, similar geometries were studied analytically for highly nonlinear systems [3]. It was found that small defects can lead to very large disturbances in the electric field, and the resulting electric field plumes are enhanced in size by a factor n in the direction perpendicular to the current flow and by a factor $\sqrt{n}$ in the parallel direction, where n is the power-law exponent of the $I-V$ characteristics. Hence the resulting electric field plume should be eccentric in shape by a factor $\sqrt{n}$, elongated in the direction perpendicular to the current flow. This anisotropic elongation is hence the cause of the eccentricity observed in the electric field plume of figure 4(b). The $I-V$ data shown in figure 2 yield a value of 26–30 for n, so the observed eccentricity of five to ten, is roughly in agreement with the expected value of $\sqrt{n}$ predicted by [3].

5. Conclusions

We have demonstrated the use of scanning potentiometry and Hall imaging for the study of local dissipation in HTS coated conductors in the presence of an applied transport current. By measuring the magnetic and electric field profiles in the vicinity of a constraining region for the current flow, we have found good agreement with recent analytical work concerning the nonlinear electrodynamics of inhomogeneous superconducting media.

Acknowledgments

This work was supported by the UK Engineering and Physical Sciences Research Council and by EU Contract BRPR CT97-0556.

References

[1] Koblishka M R and Wijngaarden R J 1995 Magneto-optical investigations of superconductors *Supercond. Sci. Technol.* **8** 199–213

[2] de Lozanne A 1999 Scanning probe microscopy of high-temperature superconductors *Supercond. Sci. Technol.* **12** 43–56

[3] Gurevich A and Friesen M 2000 Nonlinear transport current flow in superconductors with planar obstacles *Phys. Rev.* B **62** 4004

[4] Perkins G K, Bugoslavsky Yu V, Qi X, MacManus-Driscoll J L and Caplina A D 2001 High field scanning Hall probe imaging of high temperature superconductors *IEEE Trans. Appl. Supercond.* **11** 3186–9

[5] Gurevich and Kupfer H 1993 *Phys. Rev.* B **48** 6477